

## Inhibition of monoamine oxidase B by selected benzimidazole and caffeine analogues

Deidré van den Berg,<sup>a,†</sup> Kevin R. Zoellner,<sup>a,†</sup> Modupe O. Ogunrombi,<sup>a</sup> Sarel F. Malan,<sup>a</sup> Gisella Terre'Blanche,<sup>a</sup> Neal Castagnoli, Jr.,<sup>b</sup> Jacobus J. Bergh<sup>a</sup> and Jacobus P. Petzer<sup>a,\*</sup>

<sup>a</sup>Pharmaceutical Chemistry, School of Pharmacy, North-West University, Private Bag X6001, Potchefstroom 2520, South Africa

<sup>b</sup>Department of Chemistry, Virginia Tech, Blacksburg, VA 24061, USA

Received 26 January 2007; revised 11 March 2007; accepted 14 March 2007

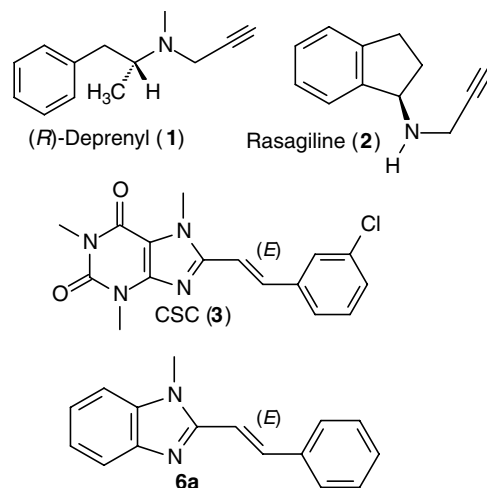
Available online 18 March 2007

**Abstract**—We have recently reported that a series of (*E*)-8-styrylcaffeines and (*E*)-2-styrylbenzimidazoles are moderate to very potent competitive inhibitors of monoamine oxidase B (MAO-B). The most potent member of the series was found to be (*E*)-8-(3-chlorostyryl)caffeine (CSC) with an enzyme-inhibitor dissociation constant ( $K_i$  value) of 128 nM. In the present study, we have prepared additional caffeine and benzimidazole analogues in an attempt to identify compounds with improved MAO-B inhibition potency while still acting reversibly. The most potent inhibitor among the caffeine analogues was (*E*)-8-(3,4-dichlorostyryl)caffeine with a  $K_i$  value of 36 nM, approximately 3.5 times more potent than CSC. The most potent inhibitor among the benzimidazole analogues was (*E*)-2-(4-trifluoromethylstyryl)-1-methylbenzimidazole with a  $K_i$  value of 430 nM. An SAR analysis indicated that the potency of MAO-B inhibition by (*E*)-2-styryl-1-methylbenzimidazole analogues depended upon the Taft steric parameter ( $E_s$ ) of the substituents attached to C-4 of the styryl phenyl ring. Substituents with a large degree of steric hindrance appear to enhance inhibition potency. The proposal that potent MAO-B inhibition by (*E*)-8-styrylcaffeines and (*E*)-2-styrylbenzimidazoles can be explained by a mode of binding that involves traversing both the entrance and substrate cavities was supported by the finding that 1-methylbenzimidazole only weakly inhibited MAO-B with a  $K_i$  value of 2084  $\mu$ M. Without the styryl side chain, 1-methylbenzimidazole is not expected to be able to bind simultaneously to both the entrance and substrate cavities.

© 2007 Elsevier Ltd. All rights reserved.

### 1. Introduction

Monoamine oxidase (MAO) is a flavin adenine dinucleotide (FAD)-containing enzyme attached to the mitochondrial outer membrane of neuronal, glial, and other cells. Its roles include regulation of the levels of biogenic and xenobiotic amines in the brain and the peripheral tissues by catalyzing their oxidative deamination.<sup>1</sup> On the basis of their substrate and inhibitor specificities, two types of MAO (A and B) have been described. MAO-A preferentially catalyzes the deamination of serotonin and norepinephrine and is irreversibly inhibited by low concentrations of clorgyline. MAO-B preferentially catalyzes the deamination of arylalkylamines such as benzylamine and is irreversibly inhibited by (*R*)-deprenyl (**1**) (Scheme 1).<sup>2</sup> Both isoforms utilize



**Scheme 1.** The structures of the mechanism-based MAO-B inactivators (*R*)-deprenyl (**1**) and Rasagiline (**2**) as well as the reversible inhibitors CSC (**3**) and (*E*)-2-styryl-1-methylbenzimidazole (**6a**).

**Keywords:** Monoamine oxidase B; Reversible inhibitors; Structure-activity relationship; Caffeine; Benzimidazole.

\* Corresponding author. Tel.: +27 18 2992206; fax: +27 18 2994243; e-mail: jacques.petzer@nwu.ac.za

<sup>†</sup> These authors contributed equally to this work.

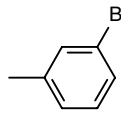
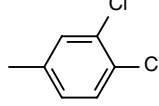
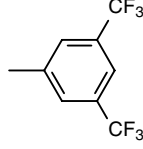
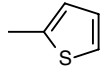
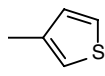
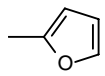
dopamine as substrate.<sup>1</sup> Due to their role in the metabolism of catecholamine neurotransmitters, MAO-A and MAO-B have long been of considerable pharmacological interest, and reversible and irreversible inhibitors of MAO-A and MAO-B have been used clinically to treat neurological disorders including depression and Parkinson's disease (PD).<sup>1</sup> MAO-B has also been implicated in neurodegenerative processes resulting from exposure to xenobiotic amines. For example, the first step of the bioactivation of the parkinsonian inducing pro-neurotoxin, 1-methyl-4-phenyl-1,2,3,6-tetrahydropyridine (MPTP), is catalyzed by MAO-B.<sup>3</sup>

MAO-A and MAO-B are therefore important targets for the development of new drugs. We are particularly interested in the therapeutic role of MAO-B inhibitors in Parkinson's disease. Since the MAO-B isoform appears to be predominantly responsible for dopamine metabolism in the basal ganglia,<sup>4,5</sup> inhibition of this enzyme in the brain may conserve the depleted supply of dopamine and inhibitors are used in combination with levodopa as dopamine replacement therapy in patients diagnosed with early PD.<sup>6</sup> MAO-B inhibitors have been shown to elevate dopamine levels in the striatum of primates treated with levodopa.<sup>7</sup> Furthermore, in the catalytic cycle of MAO, one mole of dopaldehyde and H<sub>2</sub>O<sub>2</sub> are produced for each mole of dopamine oxidized. Both these catabolic products may be neurotoxic if not rapidly inactivated by centrally located aldehyde dehydrogenase (ADH)<sup>8</sup> and glutathione peroxidase,<sup>9</sup> respectively. Thus, inhibitors of MAO-B may also exert a neuroprotective effect by stoichiometrically decreasing aldehyde and H<sub>2</sub>O<sub>2</sub> production in the brain. Inhibitors that have been demonstrated to be of clinical value include the mechanism-based inactivators, (*R*)-deprenyl<sup>10</sup> and Rasagiline (**2**)<sup>11</sup> (Scheme 1), and reversible inhibitors such as lazabemide<sup>12</sup> and safinamide.<sup>13</sup> From a safety point of view, reversible inhibitors may be therapeutically more desirable than inactivators since MAO-B activity can be regained relatively quickly following withdrawal of the reversible inhibitor. In contrast, return of enzyme activity following treatment with inactivators requires de novo synthesis of the MAO-B protein which may require several weeks.<sup>14</sup> For this reason, several studies are currently underway to develop reversible inhibitors of MAO-B.<sup>15,16</sup> These inhibitors act in a competitive manner while retaining selectivity toward MAO-B.

We have recently reported that (*E*)-8-styrylcaffeines act as moderate to very potent competitive inhibitors of MAO-B.<sup>17–19</sup> In contrast caffeine only weakly inhibited the enzyme, which indicates that substitution at C-8 enhances affinity of caffeine analogues for the active site of MAO-B. Substitution at C-8 with an electron deficient styryl functional group produced structures that were especially potent inhibitors. For example, the most potent member of the series was found to be (*E*)-8-(3-chlorostyryl)caffeine (CSC) (**3**) (Scheme 1) with an enzyme-inhibitor dissociation constant (*K*<sub>i</sub> value) of 128 nM.<sup>20</sup> A structure–activity relationship (SAR) study indicated that the structural features important for MAO-B inhibition are the *trans* configuration about the styryl

double bond and 1,3,7-trimethyl substitution of the xanthine ring. The literature supports the proposal that a wide variety of planar, heterocyclic compounds frequently act as competitive inhibitors of MAO-B. Accordingly, a small series of (*E*)-2-styrylbenzimidazoles was shown to be moderate competitive inhibitors of MAO-B.<sup>18</sup> In the present study, we have examined additional caffeine (**4a–f** and **5a–b**) and benzimidazole (**6a–g** and **7a–b**) analogues (Tables 1–4) in an attempt

**Table 1.** The *K*<sub>i</sub> values for the inhibition of MAO-B by (*E*)-8-styrylcaffeine analogues (**4a–f**)<sup>a</sup>

Compound	Ar	<i>K</i> <sub>i</sub> (μM)
<b>4a</b>		0.083
<b>4b</b>		0.036
<b>4c</b>		0.239
<b>4d</b>		1.58
<b>4e</b>		11.3
<b>4f</b>		39.7

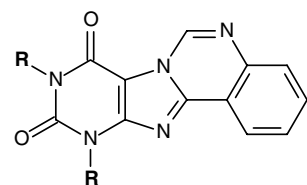
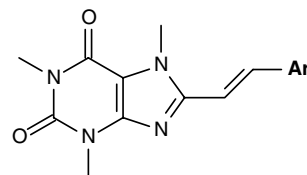
<sup>a</sup> The enzyme source used was baboon liver mitochondrial MAO-B.

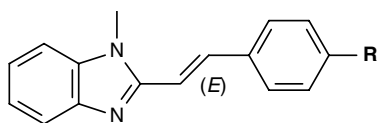
**Table 2.** The *K*<sub>i</sub> values for the inhibition of MAO-B by the purino[7,8-*c*]-quinazoline-8,10(9*H*,11*H*)-dione analogues (**5a–b**)

Compound	R	<i>K</i> <sub>i</sub> value <sup>a</sup> (μM)
<b>5a</b>	CH <sub>3</sub>	39.9
<b>5b</b>	C <sub>2</sub> H <sub>5</sub>	No inhibition <sup>b</sup>

<sup>a</sup> The enzyme source used was baboon liver mitochondrial MAO-B.

<sup>b</sup> No inhibition was observed at a maximum tested concentration of 50 μM. Due to limited solubility in the aqueous incubation solvent higher concentrations were not tested.



**Table 3.** The  $K_i$  values for the inhibition of MAO-B by (*E*)-2-styryl-1-methylbenzimidazole analogues (**6a–g**)

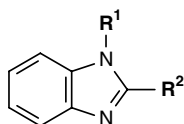
Compound	R	$K_i$ value <sup>a</sup> ( $\mu\text{M}$ )	$E_s$ <sup>b</sup>	$\pi$ <sup>b</sup>
<b>6a</b>	H	18.7, 17 <sup>c</sup>	0.00	0.00
<b>6b</b>	Cl	2.83	-0.97	0.71
<b>6c</b>	Br	2.54	-1.16	0.86
<b>6d</b>	F	14.95	-0.46	0.14
<b>6e</b>	CF <sub>3</sub>	0.43	-2.40	0.88
<b>6f</b>	CH <sub>3</sub>	3.26	-1.24	0.56
<b>6g</b>	OCH <sub>3</sub>	5.82	-0.55	-0.02

The values of the selected physicochemical parameters used in the SAR study are also listed.<sup>27</sup>

<sup>a</sup> The enzyme source used was baboon liver mitochondrial MAO-B.

<sup>b</sup> Values obtained from Ref. 27.

<sup>c</sup> Reported  $K_i$  value.<sup>18</sup>

**Table 4.** The  $K_i$  values for the inhibition of baboon liver MAO-B by methylbenzimidazoles (**7a–b**)

Compound	R <sup>1</sup>	R <sup>2</sup>	$K_i$ value ( $\mu\text{M}$ )
<b>7a</b>	CH <sub>3</sub>	H	2084
<b>7b</b>	H	CH <sub>3</sub>	1220

to identify compounds with improved MAO-B inhibition potency. Among the compounds studied was (*E*)-8-(3-bromostyryl)caffeine (**4a**). Applying a multivariate predictive equation constructed in a previous study,<sup>20</sup> this putative inhibitor is predicted to have a  $K_i$  value for the inhibition of MAO-B of 106 nM. Since electron withdrawing substituents of the styryl ring appear to enhance MAO-B inhibition potency,<sup>20</sup> we have included in this study additional (*E*)-8-styrylcaffeinyl derivatives (**4b–f**) with electron deficient styryl rings. Also studied were seven (*E*)-2-styryl-1-methylbenzimidazole analogues (**6a–g**) differing only in substitution at C-4 of the styryl phenyl ring. The principal aim with these analogues was to compare the efficacy of inhibition and possibly the binding mode of the benzimidazoles with that of the caffeine analogues. It was previously established via a Hansch-type SAR analysis that potency of MAO-B inhibition by (*E*)-8-styrylcaffeinyl analogues depended upon the descriptors of bulkiness ( $V_w$ ) and lipophilicity ( $\pi$ ) of the substituents attached to C-4 of the styryl phenyl ring.<sup>20</sup>

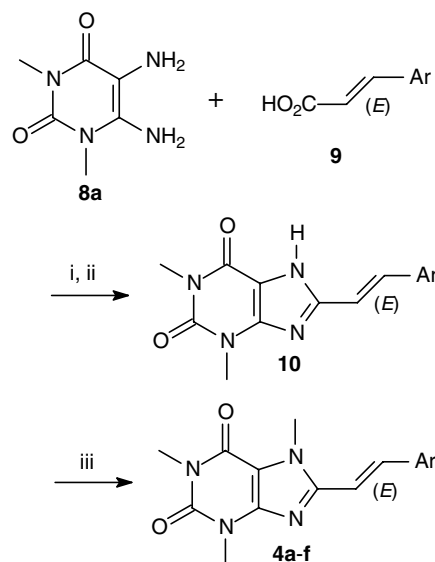
## 2. Results

### 2.1. Chemistry

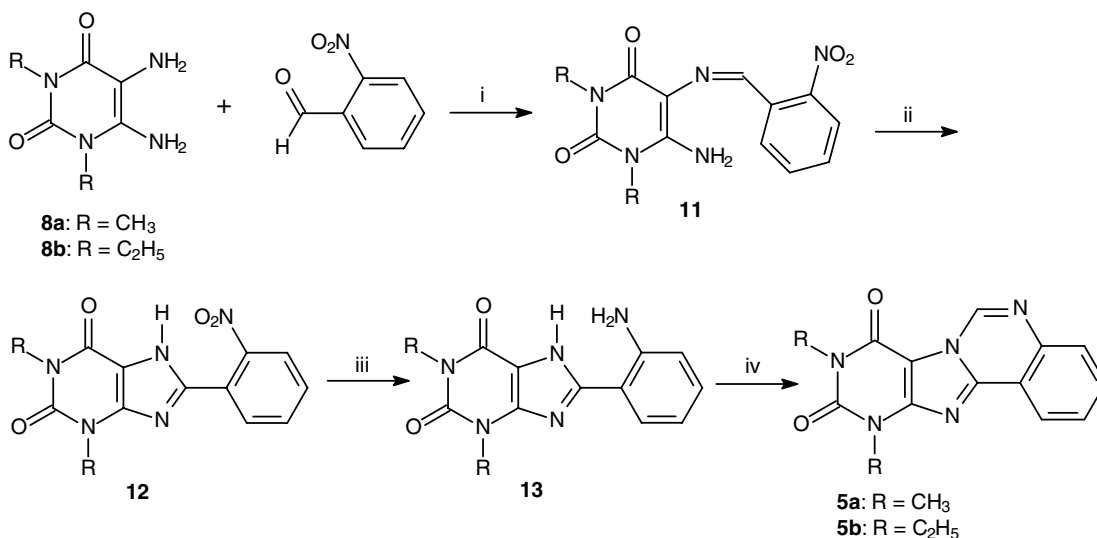
The (*E*)-8-styrylcaffeinyl analogues (**4a–f**) (Table 1) examined in this study were prepared in high yield

according to a previously reported procedure.<sup>20,21</sup> The key starting material for the procedure, 1,3-dimethyl-5,6-diaminouracil (**8a**), was allowed to react with the appropriate carboxylic acid (**9**) in the presence of a carbodiimide activating reagent (1-ethyl-2-[3-(dimethylamino)propyl]-carbodiimide, EDAC) (Scheme 2). The resulting amide intermediates underwent ring closure in refluxing aqueous sodium hydroxide to yield the corresponding 1,3-dimethyl-8-substituted-7*H*-xanthinyl analogues (**10**). Without further purification, the crude product obtained was selectively 7*N*-methylated in the presence of an excess of iodomethane and potassium carbonate to yield the target compounds **4a–f**. Following crystallization from a suitable solvent the structures and purity of all new compounds were verified by mass spectrometry, <sup>1</sup>H NMR, and <sup>13</sup>C NMR. The *trans* geometry about the styryl  $\pi$ -bonds of **4a–c** was confirmed by proton–proton coupling constants which were in the range of 15.7–15.8 Hz for the olefinic proton signals. The *trans* geometry about the ethenyl  $\pi$ -bonds of **4d–f** was confirmed by proton–proton coupling constants in the range of 15.4–15.6 Hz.

The purino[7,8-*c*]quinazoline-8,10(9*H*,11*H*)-dione analogues (**5a–b**) (Table 2) examined in this study were prepared according to a synthetic pathway reported by Ceccarelli et al. (Scheme 3).<sup>22</sup> The reaction of 1,3-dimethyl- or 1,3-diethyl-5,6-diaminouracil (**8**) with 2-nitrobenzaldehyde in the presence of acid gave 6-amino-1,3-dimethyl- or 6-amino-1,3-diethyl-5-(2-nitrobenzylideneamino)uracil (**11**) in high yields (83–89%). Oxidation of these intermediate imines with iodine in 1,2-dimethoxyethane yielded the crystalline 8-(2-nitrophenyl)-1,3-dimethyl-7*H*-xanthines (**12**). Following reduction of the nitro group with hydrochloric acid and tin powder, the resulting amines (**13**) were treated with triethyl orthoformate to yield the target compounds (**5a–b**). The structures and purity of the target



**Scheme 2.** Synthetic pathway to (*E*)-8-styrylcaffeinyl analogues (**4a–f**). Reagents and condition: (i) EDAC, dioxane/H<sub>2</sub>O; (ii) NaOH (aq), reflux; (iii) CH<sub>3</sub>I, K<sub>2</sub>CO<sub>3</sub>, DMF.



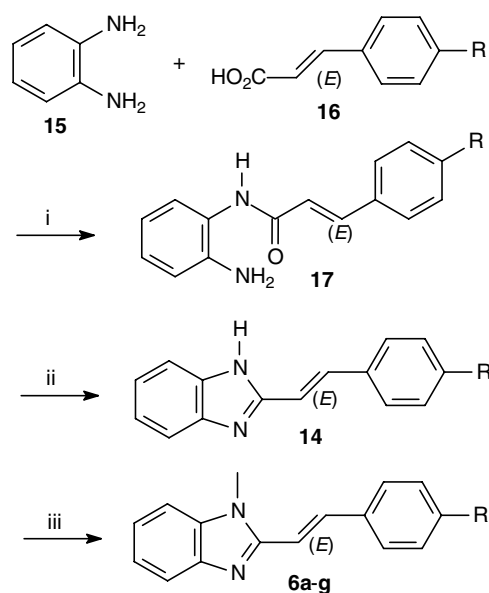
**Scheme 3.** Synthetic pathway to purino[7,8-c]quinazoline-8,10(9H,11H)-dione analogues (**5a–b**). Reagents and conditions: (i) CH<sub>3</sub>CO<sub>2</sub>H; (ii) I<sub>2</sub>, dimethoxyethane, 50 °C; (iii) Sn, HCl; (iv) HC(OC<sub>2</sub>H<sub>5</sub>)<sub>3</sub>, reflux.

compounds and intermediates were verified by their mass spectrometric, <sup>1</sup>H NMR, and <sup>13</sup>C NMR properties.

A series of (*E*)-2-styryl-1-methylbenzimidazole analogues (**6a–g**) (Table 3) also was prepared in an attempt to compare their efficacy of inhibition and possibly the binding mode to the active site with those of the caffeine analogues. Compounds **6a–g** were prepared by treating the corresponding (*E*)-2-styryl-1*H*-benzimidazole analogue (**14**) with one equivalent of iodomethane in the presence of potassium carbonate. (*E*)-2-styryl-1*H*-benzimidazole analogues have previously been prepared by reacting 2-methyl-1*H*-benzimidazole (**7b**) with an appropriately substituted benzaldehyde at high temperatures.<sup>18,23–25</sup> In this study, we have explored a different synthetic pathway to species **14** (Scheme 4) involving condensation of *o*-phenylenediamine (**15**) with an appropriately substituted cinnamic acid derivative (**16**) in the presence of the carbodiimide activating reagent (EDAC). 4-(Dimethylamino)pyridine and imidazole were used as catalysts. The resulting intermediate amide (**17**) was cyclized by heating under reflux in the presence of acid to yield the target (*E*)-2-styryl-1*H*-benzimidazole analogue (**14**) as the corresponding hydrochloric acid salt. Attempts to cyclize the intermediate amide under basic conditions resulted in hydrolysis of the amide. With the exception of **6e**, the synthesis of all the (*E*)-2-styryl-1-methylbenzimidazole analogues examined here has previously been reported. The *trans* geometry about the styryl double bonds of **6a–g** was confirmed by proton–proton coupling constants which were in the range of 15.8–15.9 Hz for the olefinic proton signals.

## 2.2. Enzymology and inhibition studies

In the present study, we have examined the possibility that the synthetic caffeine (**4a–f**, **5a–b**) and benzimidazole (**6a–g**, **7a–b**) analogues may act as inhibitors of MAO-B. The measurement of MAO-B activity in our



**Scheme 4.** Synthetic pathway to (*E*)-2-styryl-1-methylbenzimidazole analogues (**6a–g**). Reagents and condition: (i) EDAC, DMF; (ii) HCl, ethanol, reflux; (iii) CH<sub>3</sub>I, K<sub>2</sub>CO<sub>3</sub>, DMF.

laboratory is based on the MAO-B catalyzed oxidation of 1-methyl-4-(1-methylpyrrol-2-yl)-1,2,3,6-tetrahydropyridine (MMTP) to the corresponding dihydropyridinium metabolite (MMDP<sup>+</sup>).<sup>26</sup> Since MMDP<sup>+</sup> absorbs light maximally at a wavelength of 420 nm, the enzymatic production of MMDP<sup>+</sup> may be readily measured spectrophotometrically. At this wavelength neither the substrate nor the test compounds absorb light. Because of these favorable chromophoric characteristics and the *in vitro* chemical stability of MMDP<sup>+</sup>, this assay is frequently used to evaluate the potencies of potential inhibitors of MAO-B.<sup>18,20</sup> As enzyme source we have employed the mitochondrial fraction obtained from baboon liver tissue since it is reported to be devoid of

MAO-A activity while exhibiting a high degree of MAO-B catalytic activity.<sup>26</sup> Therefore, even though MMTP is a MAO-A/B mixed substrate, its oxidation by baboon liver mitochondria can be exclusively attributed to the action of the MAO-B isoform. Also, the interaction of reversible inhibitors with MAO-B obtained from baboon liver tissue appears to be similar to the interaction with the human form of the enzyme since inhibitors such as CSC are approximately equipotent with both enzyme sources.<sup>18</sup>

With the exception of **5b** all of the caffeine (**4a–f**, **5a**) and benzimidazole (**6a–g**, **7a–b**) analogues tested were found to be inhibitors of MAO-B. As demonstrated by example with (*E*)-8-(3,5-difluoromethylstyryl)caffeine (**4c**) (Fig. 1), the lines of the Lineweaver–Burk plots intersected at the *y*-axis, indicating the mode of inhibition to be competitive. The enzyme-inhibitor dissociation constants ( $K_i$  values) for the inhibition of MAO-B by the test compounds are presented in Tables 1–4. The most potent inhibitor among the caffeine analogues was found to be (*E*)-8-(3,4-dichlorostyryl)caffeine (**4b**) with a  $K_i$  value of 36 nM (Table 1), approximately 3.5 times more potent than CSC which has a reported  $K_i$  value for the inhibition of baboon liver MAO-B of 128 nM.<sup>20</sup> The second most potent inhibitor evaluated in this study was (*E*)-8-(3-bromostyryl)caffeine (**4a**), with a  $K_i$  value of 83 nM, also more potent than the lead compound CSC.

Applying a multivariate predictive equation constructed in a previous study,<sup>20</sup> we were able to predict the  $K_i$  value for the inhibition of MAO-B by **4a**. The reported electronic Hammett ( $\sigma_m$ ) parameter value and van der

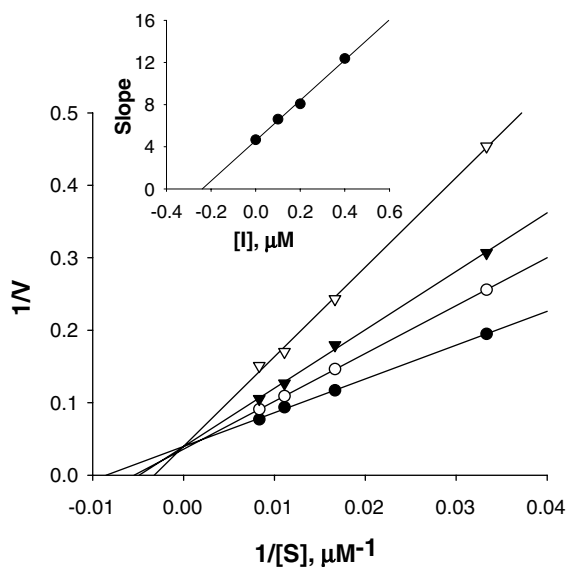


**Figure 1.** Lineweaver–Burk plots of the oxidation of MMTP by baboon liver MAO-B in the absence (filled circles) and presence of various concentrations of **4c** (open circles, 0.1  $\mu\text{M}$ ; filled triangles, 0.2  $\mu\text{M}$ ; open triangles, 0.4  $\mu\text{M}$ ). The concentration of the baboon liver mitochondrial preparation was 0.15 mg/mL and the rates are expressed as  $\text{nmol mg protein}^{-1} \text{min}^{-1}$  of  $\text{MMDP}^+$  formed. The inset is the replot of the slopes versus the inhibitor concentrations.

Waals volume ( $V_w$ ) for a bromine substituted in the meta position of a phenyl ring are 0.39 and 1.32, respectively.<sup>27,28</sup> Substitution of these values into the multivariate equation ( $\log K_i = -2.10\sigma_m - 0.49V_w + 0.49$ )<sup>20</sup> yielded a predicted  $K_i$  value of 106 nM. In spite of the few data points that were used to derive the equation, the relatively small difference between the experimentally obtained  $K_i$  value of 86 nM and the predicted value reflected the expected trend. Another inhibitor identified in this study as being exceptionally potent is (*E*)-8-(3,5-difluoromethylstyryl)caffeine (**4c**). This compound was found to inhibit MAO-B with a  $K_i$  value of 239 nM. (*E*)-8-(2-thienylethenyl)caffeine (**4d**), (*E*)-8-(3-thienylethenyl)caffeine (**4e**), and (*E*)-8-(2-furylethenyl)caffeine (**4f**) were found to be only moderate inhibitors of MAO-B with  $K_i$  values in the low micromolar range. Although only moderately potent, **4d** was still a better inhibitor than (*E*)-8-styrylcaffeine, which is reported to inhibit baboon liver MAO-B with a  $K_i$  of 2.7  $\mu\text{M}$ .<sup>20</sup> The purino[7,8-*c*]quinazoline-8,10(9*H*,11*H*)-dione analogue **5a** was found to be a weak inhibitor of MAO-B, while analogue **5b** exhibited no inhibition at concentrations up to 50  $\mu\text{M}$ , its limit of solubility in the aqueous incubation mixtures (Table 2).

The most potent inhibitor among the (*E*)-2-styryl-1-methylbenzimidazole analogues (**6a–g**) was (*E*)-2-(4-trifluoromethylstyryl)-1-methylbenzimidazole (**6e**) with a  $K_i$  value of 430 nM (Table 3). The least potent of the series was the unsubstituted (*E*)-2-styryl-1-methylbenzimidazole (**6a**) with a  $K_i$  value of 18.7  $\mu\text{M}$ . These results support evidence that substitution at the styryl phenyl ring generally leads to enhanced MAO-B inhibition activity of both (*E*)-8-styrylcaffeine and (*E*)-2-styrylbenzimidazolyl analogues. Interestingly, the electronic characteristics of the styryl substituents do not appear to correlate with inhibition activity since the analogue substituted with an electron withdrawing fluorine (**6d**) was found to be a weaker inhibitor than analogues bearing electron donating substituent (**6f–g**). On the other hand, the analogue bearing a trifluoromethyl substituent (**6e**) proved to be the most potent inhibitor in this series. This result is in agreement with a previous study which showed that MAO-B inhibition potency of (*E*)-8-styrylcaffeine analogues correlated with the size and lipophilicity of the substituent at C-4 of the styryl ring, while the contribution of electronic substituent descriptors was negligible.<sup>20</sup>

In order to quantify the relationships between MAO-B inhibitory activity of **6a–g** and the physicochemical properties of the styryl C-4 substituent, a Hansch-type SAR study was carried out by stepwise multiple linear regression analysis. Five descriptors were used to define each substituent. As descriptors of bulkiness, the van der Waals volume ( $V_w$ )<sup>28</sup> and Taft steric parameter ( $E_s$ )<sup>27</sup> were employed, while the lipophilicities of the substituents were described by the Hansch constant ( $\pi$ ).<sup>27</sup> The classical Hammett ( $\sigma_p$ ) and Swain–Lupton ( $F$ ) constants served as electronic parameters.<sup>27</sup> All physicochemical values of the substituents were obtained from standard compilations.<sup>27,28</sup> Results of the statistical analysis are presented in Table 5. The only substituent descriptor

**Table 5.** Correlations of the MAO-B inhibition constants ( $\log K_i$ ) of the (*E*)-2-styryl-1-methylbenzimidazole analogues (**6a–g**) with steric, electronic, and hydrophobic descriptors of the substituents at C-4 of the styryl ring<sup>a</sup>

Parameter	Slope	$\gamma$ -Intercept	$R^2$	$F^b$	Significance <sup>c</sup>
$\sigma_p$	$-1.33 \pm 0.67$	$0.72 \pm 0.18$	0.44	3.93	0.104
$F$	$-0.90 \pm 1.16$	$0.86 \pm 0.40$	0.11	0.60	0.47
$V_w$	$-0.69 \pm 0.37$	$1.24 \pm 0.38$	0.41	3.52	0.12
$E_s$	$0.70 \pm 0.08$	$1.28 \pm 0.09$	0.94	84.2	0.0003
$\pi$	$-1.16 \pm 0.34$	$1.12 \pm 0.19$	0.70	11.9	0.02

<sup>a</sup> The logarithm of the  $K_i$  values expressed in  $\mu\text{M}$  were used in the linear regression analysis.

<sup>b</sup> The  $F$  test statistic relates the mean squares due to regression to the error variance. Higher  $F$  values indicate a better fit and a regression equation with an  $F$  value higher than the critical  $F$  value may be judged as significant. Critical  $F$  values were calculated as described recently.<sup>29</sup>

<sup>c</sup> The significance is the fractional probability that the coefficient of the added variable is zero.

that showed a meaningful correlation with the logarithm of the  $K_i$  values (expressed in  $\mu\text{M}$ ) was the Taft steric parameter ( $E_s$ ). Regression analysis of  $\log K_i$  with  $E_s$  exhibited a relatively good correlation with a  $R^2$  value of 0.94. The statistical  $F$  value was found to be 84.2 for the correlation, a value that is larger than the critical  $F$  value (25.32) for 95% significance (a higher  $F$  value indicates a better correlation).<sup>29</sup> The confidence level of the correlation was greater than 99.9%. All other single-parameter correlations with the  $\log K_i$  values exhibited poorer statistical correlations. Therefore, the best mathematical description of the binding affinity ( $\log K_i$ ) of the C-4 substituted (*E*)-2-styryl-1-methylbenzimidazole analogues considered in this study to MAO-B is:

$$\log K_i = 0.70(\pm 0.08)E_s + 1.28(\pm 0.09) \quad (1)$$

$(F = 84.2, R^2 = 0.94 \text{ and } n = 7).$

Since larger sterically hindered substituents have increasingly negative Taft steric parameter ( $E_s$ ) values, the positive correlation observed with  $E_s$  ( $0.70 \pm 0.08$ ) indicates that the MAO-B inhibition potency ( $\log K_i$ ) may be enhanced by substitution at C-4 of the styryl ring with a sterically bulky substituent (Fig. 2). In agreement with qualitative inspection of the inhibition data presented in Table 3, the electronic contribution of the C-4 substituents to  $\log K_i$  appears to be negligible since the addition of an electronic substituent parameter

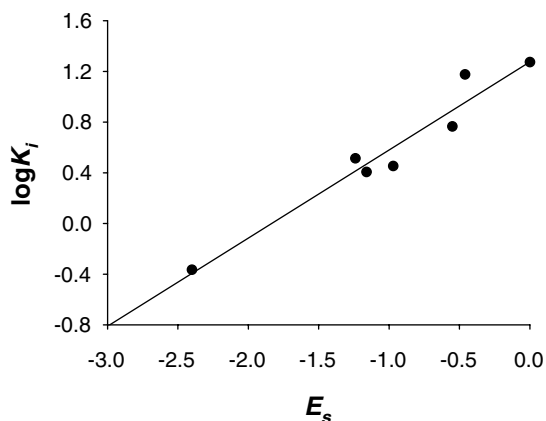
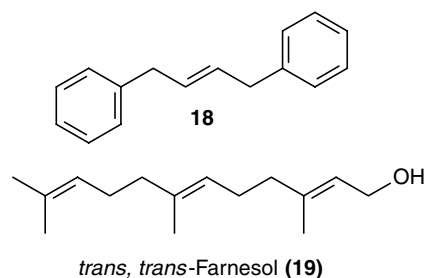


**Figure 2.** Correlation between the  $\log K_i$  values for the inhibition of MAO-B by (*E*)-2-styryl-1-methylbenzimidazole analogues (**6a–g**) and the Taft steric parameter ( $E_s$ ) of the substituents at C-4 of the styryl ring. The linear regression line is a graphical representation of Eq. 1. The correlation coefficient was found to be 0.94.

( $\sigma_p$  and  $F$ ) to the regression analysis with  $E_s$  did not improve the correlation. Although not significant, there also appears to be a moderate correlation ( $R^2 = 0.70$ ) between binding affinity ( $\log K_i$ ) and the lipophilicity ( $\pi$ ) of the C-4 substituents. Since more lipophilic substituents have increasingly positive Hansch constant ( $\pi$ ) values, the negative correlation ( $-1.16 \pm 0.34$ ) between  $\pi$  and the  $\log K_i$  values indicates that enhancement of the lipophilicity of the C-4 substituents may lead to better inhibition potency.

### 3. Discussion

The crystal structures of human recombinant MAO-B in complex with several pharmacologically important inhibitors of the enzyme have recently been reported.<sup>30–32</sup> From the surface of the enzyme, the access channel leading to the active site FAD co-factor consists of an entrance followed by a substrate cavity. An inhibitor must traverse an entrance cavity in order to gain access to the substrate cavity. This is true for small molecule inhibitors such as isatin that has been shown to bind within the substrate cavity of the enzyme.<sup>31</sup> A larger inhibitor, such as the reversible inhibitor 1,4-diphenyl-2-butene (**18**) (Scheme 5), appears to exhibit a dual binding mode that involves traversing both the entrance and substrate cavities.<sup>31</sup> Another inhibitor, *trans,trans*-farnesol (**19**), is also reported to span both the entrance and substrate cavities with the polar OH moiety in close contact with the flavin located in the substrate cavity.<sup>32</sup> The gate separating the two cavities is the side chain of Ile-199 which is thought to exhibit different rotamer conformations that allow for the fusion of the two cavities in order to accommodate



**Scheme 5.** The structures of the reversible MAO-B inhibitors 1,4-diphenyl-2-butene (**18**) and *trans,trans*-farnesol (**19**).

these larger inhibitors.<sup>32</sup> The potency of MAO-B inhibition by (*E*)-8-styrylcaffeines and (*E*)-2-styrylbenzimidazoles may possibly also be explained by a similar mode of binding that involves traversing both the entrance and substrate cavities.<sup>33</sup> These inhibitors possibly bind to MAO-B with the benzimidazole or caffeine ring located in the substrate cavity of the active site while the styryl substituent extends into the entrance cavity. In support of this hypothesis we have found 1-methylbenzimidazole (**7a**) to be a very weak inhibitor of MAO-B with a  $K_i$  value of 2084  $\mu\text{M}$  (Table 4). This inhibitor is approximately 110 times less potent than (*E*)-2-styryl-1-methylbenzimidazole (**6a**) which was found to have a  $K_i$  value of 18.7  $\mu\text{M}$  (Table 3). This difference in potency is an indication of the importance of styryl substitution for a high affinity interaction between the active site of MAO-B and the (*E*)-2-styrylbenzimidazolyl type inhibitors. Without the styryl side chain, 1-methylbenzimidazole is expected to bind to either the substrate or the entrance cavity leaving the other cavity unoccupied. Therefore, styryl substitution possibly assists with dual binding that may lead to increased inhibition potency.

The important role played by the styryl side chain is further supported by the observation that C-4 substitution of the phenyl ring has a considerable effect on the MAO-B inhibition potency of (*E*)-2-styryl-1-methylbenzimidazole analogues. Since the styryl ring of these inhibitors is thought to bind within the entrance cavity, specific interactions between the styryl substituents and amino acid side chains in the entrance cavity may explain these observations. It may be predicted that bulky and lipophilic styryl substituents may lead to increased binding affinity since the entrance cavity is lined by the side chains of hydrophobic amino acids.<sup>34</sup> In accordance with this expectation, the SAR study indicates that increasing inhibition potency correlates with increasing bulkiness ( $E_s$ ) and lipophilicity ( $\pi$ ) of the C-4 substituents. We have previously arrived at a similar conclusion as part of an SAR study with (*E*)-8-styrylcaffeine analogues bearing different substituents at C-4 of the styryl ring.<sup>20</sup> It was found that the potency of MAO-B inhibition correlated with both the size ( $V_w$ ) as well as the lipophilicity ( $\pi$ ) of the C-4 substituents. Enhancement of the size and lipophilicity of the substituents resulted in better inhibition. The similarity of the outcomes of the SAR studies with the (*E*)-2-styryl-1-methylbenzimidazole analogues and the (*E*)-8-styrylcaffeine analogues is an indication that these two types of molecules interact with the active site of the enzyme with a similar mode of binding—the benzimidazole and caffeine rings located in the substrate cavity while the styryl side chain extends into the entrance cavity. The (*E*)-8-styrylcaffeine analogues, however, have been found to be considerably more potent competitive inhibitors of MAO-B than the corresponding (*E*)-2-styryl-1-methylbenzimidazole analogues. We believe that this difference may be the result of binding interactions of the polar functional groups located on the caffeine ring (e.g., the two carbonyl oxygens) with the FAD co-factor and/or polar functionalities of the amino acids located in the substrate cavity (e.g., Tyr-398 and Tyr-435). Since the benzimidazole ring is devoid of polar functional groups, such

interactions between the substrate cavity and the benzimidazolyl analogues are not possible.

Another interesting outcome of this study was that the (*E*)-8-styrylcaffeine analogue disubstituted with chlorine at C-3 and C-4 of the styryl ring (**4b**) was found to be a more potent inhibitor ( $K_i = 36$  nM) than CSC (**3**), which is monosubstituted with chlorine at C-3 ( $K_i = 128$  nM). We have previously reported<sup>20</sup> that the (*E*)-8-styrylcaffeine analogue that is monosubstituted with chlorine at C-4 ( $K_i = 260$  nM) also inhibits MAO-B potently. This synergistic effect of disubstitution on MAO-B inhibition suggests that there exists, possibly within the entrance cavity, an aromatic binding pocket with at least two major interaction sites, one for substituents at C-3 of the aromatic ring and another for substituents at C-4. Alternatively, the addition of a second substituent may simply enhance the lipophilicity of the inhibitor and therefore its affinity for the enzyme. We have previously shown that the lipophilicity of the C-4 styryl substituents correlates with MAO-B inhibition potency of (*E*)-8-styrylcaffeines.<sup>20</sup>

#### 4. Experimental

**Caution**—MMTP is a structural analogue of the nigrostriatal neurotoxin, 1-methyl-4-phenyl-1,2,3,6-tetrahydropyridine (MPTP), and should be handled using disposable gloves and protective eyewear. Procedures for the safe handling of MPTP have been described previously.<sup>35</sup>

##### 4.1. Chemicals and instrumentation

All starting materials not described elsewhere were obtained from Sigma–Aldrich and were used without purification. 1,3-Dimethyl-5,6-diaminouracil (**8a**), 1,3-diethyl-5,6-diaminouracil (**8b**)<sup>36</sup>, and the oxalate salt of MMTP<sup>37</sup> were prepared according to previously reported procedures. Because of chemical instability, compounds **8a** and **8b** were used within 24 h of preparation. Petroleum ether used in this study was of a distillation range of 40–60 °C. Proton and carbon NMR spectra were recorded on a Varian Gemini 300 spectrometer. Proton (<sup>1</sup>H) spectra were recorded in CDCl<sub>3</sub> or DMSO-*d*<sub>6</sub> at a frequency of 300 MHz and carbon (<sup>13</sup>C) spectra at 75 MHz. Chemical shifts are reported in parts per million ( $\delta$ ) downfield from the signal of tetramethylsilane added to the deuterated solvent. Spin multiplicities are given as s (singlet), d (doublet), t (triplet), q (quartet), br s (broad singlet) or m (multiplet) and the coupling constants ( $J$ ) are given in hertz (Hz). Direct insertion electron impact ionization (EIMS) and high resolution mass spectra (HRMS) were obtained on a VG 7070E mass spectrometer. Melting points (mp) were determined on a Gallenkamp melting point apparatus or by differential scanning calorimetry (DSC) on a Shimadzu DSC-50 instrument. All the melting points are uncorrected. UV–vis spectra were recorded on a Milton-Roy Spectronic 1201 spectrophotometer. Thin layer chromatography (TLC) was carried out using silica gel 60 (Macherey-Nagel) containing UV<sub>254</sub> fluorescent indicator.

#### 4.2. General procedure for the synthesis of (*E*)-8-styryl-caffeine analogues (**4a–f**)

(*E*)-8-Styrylcaffeine analogues (**4a–f**) examined in this study were prepared according to the procedure described by Suzuki and et al.<sup>21</sup> To a solution of 1,3-dimethyl-5,6-diaminouracil (**8a**, 3.50 mmol) and 1-ethyl-2-[3-(dimethylamino)propyl]-carbodiimide hydrochloride (EDAC; 5.11 mmol) in 40 mL dioxane/H<sub>2</sub>O (1:1) was added the appropriate commercially available carboxylic acid (**9**, 3.81 mmol). The pH of the suspension was adjusted to 5 with 2 M aqueous hydrochloric acid and stirring was continued for an additional 2 h. The reaction mixture was neutralized with 1 M aqueous sodium hydroxide, cooled to 0 °C, and the resulting precipitate was collected by filtration. The crude product was dissolved in 40 mL aqueous sodium hydroxide (1 M)/dioxane (1:1) and heated for 2 h under reflux. The reaction mixture was cooled to 0 °C, acidified to a pH of 4 with 4 M aqueous hydrochloric acid, and the precipitate was collected by filtration. The resulting 1,3-methyl-(*E*)-8-styryl-7*H*-xanthinyl analogues (**10**) were used in the subsequent reaction without further purification. Iodomethane (0.40 mmol) was added to a stirred suspension of **10** (0.20 mmol) and potassium carbonate (0.50 mmol) in 5 mL DMF. Stirring was continued at 60 °C for 60 min, the insoluble materials were removed by filtration, and sufficient water was added to the filtrate to precipitate the product (**4**) that was collected by filtration. Following crystallization from a mixture of methanol/ethyl acetate (9:1) analytically pure samples of **4a–f** were obtained. For **4e** we found the melting point to be 218 °C, while the reported melting point is 216–218 °C.<sup>38</sup> NMR and MS data also correlated to the corresponding published data.

(*E*)-8-(3-Bromostyryl)caffeine (**4a**) was prepared from 1,3-dimethyl-5,6-diaminouracil (**8a**) and *trans*-3-bromocinnamic acid in a yield of 37%: mp 229–231 °C (capillary method); <sup>1</sup>H NMR (CDCl<sub>3</sub>) δ 3.38 (s, 3H), 3.59 (s, 3H), 4.05 (s, 3H), 6.88 (d, 1H, *J* = 15.8 Hz), 7.25 (m, 1H), 7.45 (dd, 2H, *J* = 1.7, 7.9 Hz), 7.70 (d, 1H, *J* = 15.7 Hz), 7.71 (t, 1H, *J* = 1.8 Hz); <sup>13</sup>C NMR (CDCl<sub>3</sub>) δ 27.92, 29.72, 31.55, 108.12, 112.59, 123.12, 126.16, 129.81, 130.42, 132.21, 136.48, 137.64, 148.52, 149.30, 151.65, 155.24; EIMS *m/z* 374 and 376 (M<sup>+</sup>); HRMS calcd 374.0378, found 374.0371.

(*E*)-8-(3,4-Dichlorostyryl)caffeine (**4b**) was prepared from 1,3-dimethyl-5,6-diaminouracil (**8a**) and *trans*-3,4-dichlorocinnamic acid in a yield of 42%: mp >240 °C (capillary method); <sup>1</sup>H NMR (CDCl<sub>3</sub>) δ 3.39 (s, 3H), 3.60 (s, 3H), 4.06 (s, 3H), 6.87 (d, 1H, *J* = 15.7 Hz), 7.37 (m, 1H), 7.45 (d, 1H, *J* = 8.4 Hz), 7.64 (d, 1H, *J* = 2.1 Hz), 7.68 (d, 1H, *J* = 15.7 Hz); <sup>13</sup>C NMR (CDCl<sub>3</sub>) δ 27.93, 29.72, 31.56, 108.18, 112.91, 126.46, 128.68, 130.89, 133.24, 133.28, 135.40, 135.57, 148.49, 149.07, 151.62, 155.22; EIMS *m/z* 365 (M<sup>+</sup>); HRMS calcd 364.0494, found 364.0513.

(*E*)-8-(3,5-Ditri-fluoromethylstyryl)caffeine (**4c**) was prepared from 1,3-dimethyl-5,6-diaminouracil (**8a**) and *trans*-3,5-ditri-fluoromethylcinnamic acid in a yield of 38%: mp 267–268 °C (capillary method); <sup>1</sup>H NMR

(CDCl<sub>3</sub>) δ 3.39 (s, 3H), 3.60 (s, 3H), 4.10 (s, 3H), 7.03 (d, 1H, *J* = 15.8 Hz), 7.82 (br s, 1H), 7.84 (d, 1H, *J* = 15.8 Hz), 7.96 (br s, 2H); <sup>13</sup>C NMR (CDCl<sub>3</sub>) δ 27.96, 29.71, 31.70, 108.49, 114.84, 122.42, 124.89, 126.90, 132.48 (q), 134.53, 137.62, 148.44, 148.47, 151.60, 155.25; EIMS *m/z* 432 (M<sup>+</sup>); HRMS calcd 432.1021, found 432.1001.

(*E*)-8-(2-Thienylethenyl)caffeine (**4d**) was prepared from 1,3-dimethyl-5,6-diaminouracil (**8a**) and 3-(2-thienyl)acrylic acid in a yield of 32%: mp 204 °C (capillary method); <sup>1</sup>H NMR (CDCl<sub>3</sub>) δ 3.36 (s, 3H), 3.57 (s, 3H), 3.99 (s, 3H), 6.63 (d, 1H, *J* = 15.4 Hz), 7.03 (dd, 1H, *J* = 5.1, 5.1 Hz), 7.21 (d, 1H, *J* = 4.8 Hz), 7.30 (d, 1H, *J* = 5.1 Hz), 7.86 (d, 1H, *J* = 15.4 Hz); <sup>13</sup>C NMR (CDCl<sub>3</sub>) δ 27.86, 29.67, 31.44, 107.82, 110.21, 127.02, 128.14, 129.46, 130.89, 140.84, 148.53, 149.65, 151.62, 155.09; EIMS *m/z* 302 (M<sup>+</sup>); HRMS calcd 302.0837, found 302.0820.

(*E*)-8-(2-Furylethenyl)caffeine (**4f**) was prepared from 1,3-dimethyl-5,6-diaminouracil (**8a**) and 3-(2-furyl)acrylic acid in a yield of 35%: mp >240 °C (capillary method); <sup>1</sup>H NMR (CDCl<sub>3</sub>) δ 3.35 (s, 3H), 3.56 (s, 3H), 3.98 (s, 3H), 6.44 (m, 1H), 6.52 (d, 1H, *J* = 3.92 Hz), 6.75 (d, 1H, *J* = 15.5 Hz), 7.44 (d, 1H, *J* = 2.3 Hz), 7.72 (d, 1H, *J* = 6.32 Hz), 7.50 (d, 1H, *J* = 15.5 Hz); <sup>13</sup>C NMR (CDCl<sub>3</sub>) δ 27.84, 29.63, 31.37, 107.86, 109.11, 112.34, 113.12, 124.63, 143.87, 148.55, 149.86, 151.63, 151.79, 155.08; EIMS *m/z* 286 (M<sup>+</sup>); HRMS calcd 286.1066, found 286.1064.

#### 4.3. Synthesis of purino[7,8-*c*]quinazoline-8,10(9*H*,11*H*)-dione analogues (**5a–b**)

The purino[7,8-*c*]quinazoline-8,10(9*H*,11*H*)-dione analogues (**5a–b**) examined here were prepared from the corresponding 1,3-dialkyl-5,6-diaminouracil (**8a–b**) and 2-nitrobenzaldehyde according to the synthetic pathway reported by Ceccarelli et al. (Scheme 3).<sup>22</sup> For **5a** the melting point was found to be 258.3 °C (DSC) which is lower than the reported value of 276.1 °C.<sup>22</sup> The NMR and MS data however were fully consistent with the structure.

Purino[7,8-*c*]quinazoline-8,10(9*H*,11*H*)-dione analogue **5b** was prepared from 8-(2-aminophenyl)-1,3-diethyl-7*H*-xanthine (**13b**) in a yield of 82.9%: mp 238.2 °C (chloroform); <sup>1</sup>H NMR (DMSO-*d*<sub>6</sub>) δ 1.21 (t, 3H, *J* = 7.0 Hz), 1.35 (t, 3H, *J* = 7.1 Hz), 4.02 (q, 2H, *J* = 6.9 Hz), 4.23 (q, 2H, *J* = 7.0 Hz), 7.84 (t, 1H, *J* = 6.8, 7.9 Hz), 7.96 (t, 1H, *J* = 6.7, 7.0 Hz), 8.07 (d, 1H, *J* = 8.1 Hz), 8.53 (d, 1H, *J* = 8.2 Hz), 9.51 (s, 1H); <sup>13</sup>C NMR (DMSO-*d*<sub>6</sub>) δ 13.13, 13.25, 35.94, 38.63, 101.68, 117.48, 123.56, 128.52, 129.25, 132.51, 136.45, 142.13, 145.78, 149.82, 150.22, 153.89; HRMS calcd 309.1226, found 309.1209.

#### 4.4. General procedure for the synthesis of (*E*)-2-styryl-1-methylbenzimidazole analogues (**6a–g**)

To a solution of *o*-phenylenediamine (**15**) (10 mmol) and EDAC (15 mmol) in DMF (10–15 mL) was added the

appropriately substituted cinnamic acid derivative (**16**) (10 mmol). 4-(Dimethylamino)pyridine (0.05 equiv) and imidazole (0.05 equiv) were added as catalysts and the reaction was stirred at room temperature for 4 h. Water (150 mL) then was added to the reaction mixture and the resulting precipitate was collected by filtration. This intermediate amide (**17**) was suspended in 20 mL of 6 M aqueous hydrochloric acid, heated to 90–100 °C under reflux, and a sufficient amount of ethanol was added carefully to dissolve the amide. Heating was continued until TLC (ethyl acetate/petroleum ether, 1:1) indicated completion of the reaction. The reaction mixture was cooled to 0 °C and the precipitate that formed was collected by filtration and washed with water. These (*E*)-2-styryl-1*H*-benzimidazole analogues (**14**) were crystallized from ethanol as the corresponding hydrochloric acid salts. The yields of **14** were recorded as 24–82%. The salts (4 mmol) were dissolved in a minimal amount of DMF (5–10 mL) followed by the addition of potassium carbonate (10 mmol). The suspension was cooled to 0 °C and iodomethane (4 mmol) was added. The reaction mixture was allowed to return to room temperature and stirring was continued until TLC (ethyl acetate/dichloromethane, 1:1) indicated completion of the reaction. Except for compounds **6a** and **6f–g**, the final product was isolated by the addition of water (100 mL). The precipitate that formed was collected via filtration and crystallized from an appropriate solvent. In the cases of **6a** and **6f–g**, the remaining DMF solvent was removed via vacuum distillation. The residue was either extracted to chloroform (3 × 30 mL) or directly crystallized using an appropriate solvent. The melting points of compounds reported previously were as follows: **6a** mp 121–122 °C (from toluene, capillary method), lit. mp 119–121 °C;<sup>18</sup> **6b** mp 155 °C (from ethyl acetate/dichloromethane, 1:1), lit. mp 145–146 °C;<sup>23</sup> **6c** mp 161 °C (from ethyl acetate/dichloromethane, 1:1), lit. mp 152–153 °C;<sup>23</sup> **6d** mp 113 °C (from ethyl acetate/dichloromethane, 1:1), lit. mp 116–118 °C;<sup>23</sup> **6f** mp 108 °C (from acetonitrile), lit. mp 130–131 °C;<sup>23</sup> **6g** mp 133 °C (from acetonitrile), lit. mp 125–126 °C.<sup>23</sup> The characterization of previously unreported **6e** is summarized below.

(*E*)-2-(4-Trifluoromethylstyryl)-1-methylbenzimidazole (**6e**). Following crystallization from ethyl acetate/dichloromethane (1:1) light yellow crystals were obtained in a yield of 42.8%; mp 127 °C (capillary method); <sup>1</sup>H NMR (DMSO-*d*<sub>6</sub>) δ 3.94 (s, 3H), 7.22 (m, 2H), 7.52 (m, 1H), 7.62 (m, 1H), 7.66 (d, 1H, *J* = 15.8 Hz), 7.76 (d, 2H, *J* = 8.2 Hz), 7.89 (d, 1H, *J* = 15.8 Hz), 8.02 (d, 2H, *J* = 8.2 Hz); <sup>13</sup>C NMR (*d*<sub>6</sub>-DMSO) δ 29.59, 110.22, 117.27, 118.61, 122.17, 122.25, 125.53 (q), 127.93, 128.30, 128.72, 133.91, 136.06, 140.00, 142.73, 150.31; HRMS calcd 302.1031, found 302.1043.

#### 4.5. Synthesis of 1-methylbenzimidazole (**7a**) and 2-methyl-1*H*-benzimidazole (**7b**)

1-Methylbenzimidazole (**7a**) was synthesized from benzimidazole according to the literature procedure reported for the synthesis of 1,2-dimethylbenzimidazole.<sup>39</sup> The crude product was purified with a VersaFlash station

equipped with a 75 mm silica Versapak cartridge using dichloromethane/ethylacetate/methanol (10:10:2) as mobile phase. The melting point was found to be 54–57 °C (capillary method) which corresponded with the reported value of 57–60 °C.<sup>40</sup> <sup>1</sup>H NMR (DMSO-*d*<sub>6</sub>) δ 3.81 (s, 3H), 7.23 (m, 2H), 7.58 (m, 1H), 7.66 (m, 1H), 8.17 (s, 1H); <sup>13</sup>C NMR (DMSO-*d*<sub>6</sub>) δ 30.54, 110.05, 119.23, 121.34, 122.15, 134.54, 143.31, 144.46; HRMS calcd 132.0687, found 132.0691.

2-Methyl-1*H*-benzimidazole (**7b**) was synthesized according to Phillips<sup>41</sup> by condensing *o*-phenylenediamine with acetic acid. The melting point was found to be 175–176 °C (capillary method) which corresponded with the reported value of 176 °C.<sup>41</sup> <sup>1</sup>H NMR (DMSO-*d*<sub>6</sub>) δ 2.50 (s, 3H), 7.11 (m, 2H), 7.47 (m, 2H), 10.92 (br s, 1H); <sup>13</sup>C NMR (DMSO-*d*<sub>6</sub>) δ 14.57, 114.16, 120.97, 121.01, 138.93, 151.20; HRMS calcd 132.0687, found 132.0681.

#### 4.6. MAO-B inhibition studies

Mitochondria were isolated from baboon liver tissue as described previously<sup>42</sup> and stored at –70 °C in 300 μL aliquots. Following addition of an equal volume of sodium phosphate buffer (100 mM, pH 7.4) containing glycerol (50%, w/v) to the aliquots, the protein concentration was determined by the method of Bradford using bovine serum albumin as reference standard.<sup>43</sup> Since the mitochondrial fraction obtained from baboon liver tissue is reported to be devoid of MAO-A activity,<sup>26</sup> inactivation of this enzyme was unnecessary. The MAO-A and -B mixed substrate MMTP (*K*<sub>m</sub> = 60.9 μM for baboon liver MAO-B)<sup>26</sup> served as substrate for the inhibition studies. Incubations were carried out in sodium phosphate buffer (100 mM, pH 7.4) and contained MMTP (30–120 μM), the mitochondrial isolate (0.15 mg protein/mL), and various concentrations of the test inhibitors. The final volume of the incubations was 500 μL. The stock solutions of the inhibitors were prepared in DMSO and were added to the incubation mixtures to yield a final DMSO concentration of 4% (v/v). DMSO concentrations higher than 4% are reported to inhibit MAO-B.<sup>15</sup> Following incubation at 37 °C for 15 min, the enzyme reactions were terminated by the addition of 10 μL perchloric acid (70%) and the samples were centrifuged at 16,000*g* for 10 min. The MAO-B catalyzed production of MMDP<sup>+</sup> is reported to be linear for the first 15 min of incubation under these conditions.<sup>26</sup> The supernatant fractions were removed and the concentrations of the MAO-B generated product, MMDP<sup>+</sup>, were measured spectrophotometrically at 420 nm ( $\epsilon = 25,000 \text{ M}^{-1}$ ).<sup>26</sup> The initial rates of oxidation at four different substrate concentrations (30–120 μM) in the absence and presence of three different concentrations of the inhibitors were calculated and Lineweaver–Burk plots were constructed. The slopes of the Lineweaver–Burk plots were plotted versus the inhibitor concentration and the *K*<sub>i</sub> value was determined from the *x*-axis intercept (intercept = –*K*<sub>i</sub>). Linear regression analysis was performed using the SigmaPlot software package (Systat Software Inc.). Each *K*<sub>i</sub> value reported here is representative of a single determination

where the correlation coefficient ( $R^2$  value) of the replot of the slopes versus the inhibitor concentrations was at least 0.98.

#### 4.7. SAR study

The values of the substituent descriptors  $\sigma_p$ ,  $F$ ,  $\pi$ , and  $E_s$  were obtained from Hansch and Leo<sup>27</sup>, while those for the van der Waals volume ( $V_w$ ) were obtained from compilations by Van de Waterbeemb and Testa.<sup>28</sup> Linear regression analysis of the  $\log K_i$  values as a function of the substituent descriptor values was carried out with Statistica software package (StatSoft Inc.). In order to estimate the significance of the regression equations the  $F$  statistic was employed. An  $F$  value higher than the critical  $F$  value was judged to be significant and critical  $F$  values were calculated as described recently.<sup>29</sup> The critical  $F$  value ( $F_{\max}$ ) for 95% significance for models constructed from seven  $\log K_i$  values (Table 3) and which contains one parameter (out of a possible five:  $V_w$ ,  $E_s$ ,  $\pi$ ,  $\sigma_p$ ,  $F$ ) was calculated to be 25.32.

#### Acknowledgments

We are grateful to Jan du Preez and the staff of the Analytical Technology Laboratory, North-West University, for their support. The NMR and MS spectra were recorded by André Joubert, Johan Jordaan, and Louis Fourie of the SASOL Centre for Chemistry, North-West University. This work was supported by grants from the National Research Foundation and the Medical Research Council, South Africa.

#### References and notes

1. Youdim, M. B. H.; Bakhle, Y. S. *Br. J. Pharmacol.* **2006**, *147*, S287.
2. Waldmeier, P. C. *J. Neural Transm. Suppl.* **1987**, *23*, 55.
3. Chiba, K.; Trevor, A. J.; Castagnoli, N., Jr. *Biochem. Biophys. Res. Commun.* **1984**, *120*, 574.
4. Collins, G. G. S.; Sandler, M.; Williams, E. D.; Youdim, M. B. H. *Nature* **1970**, *225*, 817.
5. Youdim, M. B. H.; Collins, G. G. S.; Sandler, M.; Bevan-Jones, A. B.; Pare, C. M.; Nicholson, W. J. *Nature* **1972**, *236*, 225.
6. Birkmayer, W.; Riederer, P.; Youdim, M. B. H.; Linauer, W. J. *J. Neural Transm.* **1975**, *36*, 303.
7. Finberg, J. P.; Wang, J.; Bankiewicz, K.; Harvey-White, J.; Kopin, I. J.; Goldstein, D. S. *J. Neural Transm. Suppl.* **1998**, *52*, 279.
8. Gesi, M.; Santinami, A.; Ruffoli, R.; Conti, G.; Fornai, F. *Pharmacol. Toxicol.* **2001**, *89*, 217.
9. Gotz, M. E.; Freyberger, A.; Riederer, P. *J. Neural Transm. Suppl.* **1990**, *29*, 241.
10. Ebadi, M.; Brown-Borg, H.; Ren, J.; Sharma, S.; Shavali, S.; El ReFaey, H.; Carlson, E. C. *Curr. Drug Targets* **2006**, *7*, 1513.
11. Rabey, J. M.; Sagi, L.; Huberman, M.; Melamed, E.; Korczyn, A.; Giladi, M.; Inzelberg, R.; Djaldetti, R.; Klein, C.; Berecz, G. *Clin. Neuropharmacol.* **2000**, *23*, 324.
12. Dingemans, J.; Wood, N.; Jorga, K.; Kettler, R. *Br. J. Clin. Pharmacol.* **1997**, *43*, 41.
13. Chazot, P. L. *Curr. Opin. Investig. Drugs* **2001**, *2*, 809.
14. Thebault, J. J.; Guillaume, M.; Levy, R. *Pharmacotherapy* **2004**, *24*, 1295.
15. Gnerre, C.; Catto, M.; Leonetti, F.; Weber, P.; Carrupt, P.-A.; Altomare, C.; Carotti, A.; Testa, B. *J. Med. Chem.* **2000**, *43*, 4747.
16. Chimenti, F.; Maccioni, E.; Secci, D.; Bolasco, A.; Chimenti, P.; Granese, A.; Befani, O.; Turini, P.; Alcaro, S.; Ortuso, F.; Cirilli, R.; La Torre, F.; Cardia, M. C.; Distinto, S. *J. Med. Chem.* **2005**, *48*, 7113.
17. Chen, J. F.; Xu, K.; Petzer, J. P.; Staal, R.; Xu, Y. H.; Beilstein, M.; Sonsalla, P. K.; Castagnoli, K.; Castagnoli, N., Jr.; Schwarzschild, M. A. *J. Neurosci.* **2001**, *21*, RC143.
18. Petzer, J. P.; Steyn, S.; Castagnoli, K. P.; Chen, J. F.; Schwarzschild, M. A.; Van der Schyf, C. J.; Castagnoli, N., Jr. *Bioorg. Med. Chem.* **2003**, *11*, 1299.
19. Castagnoli, N., Jr.; Petzer, J. P.; Steyn, S.; Castagnoli, K.; Chen, J. F.; Schwarzschild, M. A.; Van der Schyf, C. J. *Neurology* **2003**, *61*(Suppl. 6), S62.
20. Vlok, N.; Malan, S. F.; Castagnoli, N., Jr.; Bergh, J. J.; Petzer, J. P. *Bioorg. Med. Chem.* **2006**, *14*, 3512.
21. Suzuki, F.; Shimada, J.; Shiozaki, S.; Ichikawa, S.; Ishii, A.; Nakamura, J.; Nonaka, H.; Kobayashi, H.; Fuse, E. *J. Med. Chem.* **1993**, *36*, 2508.
22. Ceccarelli, S.; D'Alessandro, A.; Magnante, F.; Scuri, R.; Zanarella, S. *Farmaco* **1993**, *48*, 1301.
23. Pushkina, L. N.; Mazalov, S. A.; Postovskii, I. Y. *J. Gen. Chem. USSR (Engl. Transl.)* **1962**, *32*, 2585.
24. Dubey, P. K.; Kumar, R.; Chameron, T. S.; Grossert, J. S.; Hooper, D. L. *Indian J. Chem., Sect B* **1999**, *38*, 914.
25. Ramaiah, K.; Dubey, P. K.; Eswara, R. D.; Ramanatham, J.; Ramesh, K.; Grossert, J. S.; Hooper, D. L. *Indian J. Chem., Sect B* **2000**, *39*, 904.
26. Inoue, H.; Castagnoli, K.; Van der Schyff, C. J.; Mabic, S.; Igarashi, K.; Castagnoli, N., Jr. *J. Pharmacol. Exp. Ther.* **1999**, *291*, 856.
27. Hansch, C.; Leo, A. *Exploring QSAR. Fundamentals and Applications in Chemistry and Biology*; American Chemical Society: Washington, DC, 1995, pp 1–124.
28. Van de Waterbeemb, H.; Testa, B. In *Advances in Drug Research*; Testa, B., Ed.; Academic Press: London, 1987; pp 85–225.
29. Livingstone, D. J.; Salt, D. W. *J. Med. Chem.* **2005**, *48*, 661.
30. Binda, C.; Hubálek, F.; Li, M.; Herzig, Y.; Sterling, J.; Edmondson, D. E.; Mattevi, A. *J. Med. Chem.* **2004**, *47*, 1767.
31. Binda, C.; Hubálek, F.; Restelli, N.; Edmondson, D. E.; Mattevi, A. *Proc. Natl. Acad. Sci. U.S.A.* **2003**, *100*, 9750.
32. Hubálek, F.; Binda, C.; Khalil, A.; Li, M.; Mattevi, A.; Castagnoli, N., Jr.; Edmondson, D. E. *J. Biol. Chem.* **2005**, *280*, 15761.
33. Binda, C.; Hubálek, F.; Li, M.; Castagnoli, N.; Edmondson, D. E.; Mattevi, A. *Neurology* **2006**, *67*, S5.
34. Binda, C.; Newton-Vinson, P.; Hubálek, F.; Edmondson, D. E.; Mattevi, A. *Nat. Struct. Biol.* **2002**, *9*, 22.
35. Pitts, S. M.; Markey, S. P.; Murphy, D. L.; Weisz, A. In *MPTP: A Neurotoxin Producing a Parkinsonian Syndrome*; Markey, S. P., Castagnoli, N., Jr., Trevor, A. J., Kopin, I. J., Eds.; Academic Press: New York, 1986; pp 703–716.
36. Blicke, F. F.; Godt, H. C., Jr. *J. Am. Chem. Soc.* **1954**, *76*, 2798.
37. Bissel, P.; Bigley, M. C.; Castagnoli, K.; Castagnoli, N., Jr. *Bioorg. Med. Chem.* **2002**, *10*, 3031.
38. Del Giudice, M. R.; Borioni, A.; Mustazza, C.; Gatta, F.; Dionisotti, S.; Zocchi, C.; Ongini, E. *Eur. J. Med. Chem.* **1996**, *31*, 59.

39. Gazit, A.; Yee, K.; Uecker, A.; Böhmer, F. D.; Sjöblom, T.; Ostman, A.; Waltenberger, J.; Golomb, G.; Banai, S.; Heinrich, M. C.; Levitzki, A. *Bioorg. Med. Chem.* **2003**, *11*, 2007.
40. Bergman, J.; Sand, P. *Tetrahedron Lett.* **1984**, *25*, 1957.
41. Phillips, M. A. *J. Chem. Soc.* **1928**, *2*, 2393.
42. Salach, J. I.; Weyler, W. *Methods Enzymol.* **1987**, *142*, 627.
43. Bradford, M. M. *Anal. Biochem.* **1976**, *72*, 248.